

Provided for non-commercial research and education use.  
Not for reproduction, distribution or commercial use.



This article appeared in a journal published by Elsevier. The attached copy is furnished to the author for internal non-commercial research and education use, including for instruction at the authors institution and sharing with colleagues.

Other uses, including reproduction and distribution, or selling or licensing copies, or posting to personal, institutional or third party websites are prohibited.

In most cases authors are permitted to post their version of the article (e.g. in Word or Tex form) to their personal website or institutional repository. Authors requiring further information regarding Elsevier's archiving and manuscript policies are encouraged to visit:

<http://www.elsevier.com/copyright>

Contents lists available at [ScienceDirect](http://www.sciencedirect.com)

NeuroImage

journal homepage: [www.elsevier.com/locate/ynimg](http://www.elsevier.com/locate/ynimg)

## Reduced cognitive control of response inhibition by the anterior cingulate cortex in autism spectrum disorders

Yigal Agam<sup>a,b,c</sup>, Robert M. Joseph<sup>d</sup>, Jason J.S. Barton<sup>e</sup>, Dara S. Manoach<sup>a,b,c,\*</sup>

<sup>a</sup> Department of Psychiatry, Massachusetts General Hospital, Harvard Medical School, Boston, MA 02215, USA

<sup>b</sup> Athinoula A. Martinos Center for Biomedical Imaging, Charlestown, MA 02129, USA

<sup>c</sup> Harvard Medical School, Boston, MA 02215, USA

<sup>d</sup> Department of Anatomy and Neurobiology, Boston University School of Medicine, Boston, MA, USA

<sup>e</sup> Departments of Neurology, Ophthalmology and Visual Sciences, University of British Columbia, Vancouver, BC, Canada

### ARTICLE INFO

#### Article history:

Received 16 December 2009

Revised 27 March 2010

Accepted 3 April 2010

Available online 13 April 2010

### ABSTRACT

Response inhibition, or the suppression of prepotent, but contextually inappropriate behaviors, is essential to adaptive, flexible responding. In autism spectrum disorders (ASD), difficulty inhibiting prepotent behaviors may contribute to restricted, repetitive behavior (RRB). Individuals with ASD consistently show deficient response inhibition while performing antisaccades, which require one to inhibit the prepotent response of looking towards a suddenly appearing stimulus (i.e., a prosaccade), and to substitute a gaze in the opposite direction. Here, we used fMRI to identify the neural correlates of this deficit. We focused on two regions that are critical for saccadic inhibition: the frontal eye field (FEF), the key cortical region for generating volitional saccades, and the dorsal anterior cingulate cortex (dACC), which is thought to exert top-down control on the FEF. We also compared ASD and control groups on the functional connectivity of the dACC and FEF during saccadic performance. In the context of an increased antisaccade error rate, ASD participants showed decreased functional connectivity of the FEF and dACC and decreased inhibition-related activation (based on the contrast of antisaccades and prosaccades) in both regions. Decreased dACC activation correlated with a higher error rate in both groups, consistent with a role in top-down control. Within the ASD group, increased FEF activation and dACC/FEF functional connectivity were associated with more severe RRB. These findings demonstrate functional abnormalities in a circuit critical for volitional ocular motor control in ASD that may contribute to deficient response inhibition and to RRB. More generally, our findings suggest reduced cognitive control over behavior by the dACC in ASD.

© 2010 Elsevier Inc. All rights reserved.

Autism spectrum disorders (ASD) are common neurodevelopmental disorders that are characterized by restricted, repetitive behavior (RRB) and marked impairments in socialization and communication. These three symptom clusters are thought to arise from distinct genetic and cognitive mechanisms (Happé et al., 2006; London, 2007), but these mechanisms are not well understood. Accumulating evidence suggests that executive function deficits contribute to these core symptoms of ASD (Hill, 2004; Lopez et al., 2005; South et al., 2007). Response inhibition, or the suppression of prepotent, but contextually inappropriate behaviors, is an executive function that is essential to adaptive, flexible responding. Difficulty inhibiting prepotent behaviors in favor of more contextually appropriate ones may contribute to behavior that is rigid and stereotyped, rather than flexible and responsive to contingency. Individuals with ASD, consistently show deficient inhibition during antisaccade performance (Goldberg et al., 2002; Luna et al., 2007;

Manoach et al., 2004, 1997; Minshew et al., 1999; Mosconi et al., 2009). Antisaccades require the inhibition of the prepotent response of looking towards a suddenly appearing visual stimulus (i.e., a prosaccade), and the substitution of the novel response of looking in the opposite direction (Hallett, 1978). The higher rate of antisaccade errors in ASD (i.e., looking towards rather than away from the stimulus) was recently found to correlate with the severity of RRB (Mosconi et al., 2009). In spite of the consistency of the saccadic inhibition deficit in ASD, there are presently no published reports examining its neural correlates with neuroimaging techniques. In the present study, we used an antisaccade paradigm, functional MRI (fMRI), and functional connectivity analyses, to investigate the neural correlates of response inhibition deficits in ASD and their relation to RRB. Given the lack of clear neurobiological or genetic distinctions between the diagnostic subgroups of ASD (autism, Asperger's Disorder, and Pervasive Developmental Disorder, not otherwise specified, Geschwind, 2009) and because increased antisaccade error rates have been observed across the spectrum, we did not restrict our sample to a particular diagnostic subgroup. Instead, we examined the extent to which RRB, a core feature of ASD, accounted for variability in our outcome measurements.

\* Corresponding author. 149 13th St., Room 2608, Charlestown, MA 02129, USA. Fax: +1 617 726 4078.

E-mail address: [dara@nmr.mgh.harvard.edu](mailto:dara@nmr.mgh.harvard.edu) (D.S. Manoach).

We focused on two regions that are critically involved in saccadic inhibition. First, we examined the frontal eye field (FEF), which is the key cortical region involved in generating volitional saccades (Pierrot-Deseilligny et al., 1995). In fMRI studies, the FEF consistently shows increased activation for antisaccades vs. prosaccades (e.g., Connolly et al., 2002; Ford et al., 2005; Manoach et al., 2007; O'Driscoll et al., 1995; Sweeney et al., 1996), which predicts longer saccadic latencies (Connolly et al., 2002). This increased activation is thought to reflect a heightened level of inhibition that suppresses the dominant prosaccade response (DeSouza et al., 2003; Ford et al., 2009; Manoach et al., 2007). In monkey neurophysiology studies, in contrast, there is reduced preparatory activity of the FEF for antisaccades compared with prosaccades, which correlates with longer latencies and lower error rates (Everling and Munoz, 2000). Presumably, on antisaccade trials decreased preparatory activity in the FEF results in a longer latency to reach the threshold for triggering a saccade, and also makes it harder for the dominant prosaccade to escape (Everling and Munoz, 2000). Thus both decreased neuronal spiking and increased BOLD activation for antisaccades vs. prosaccades are hypothesized to reflect inhibition of the FEF. The seeming discrepancy in the direction of activity change likely arises from the different sources of signals in these two techniques (Ford et al., 2009): one potential interpretation is that increased fMRI activation reflects a heightened level of inhibitory input and/or increased activity of local inhibitory interneurons, which could then account for the reduced spiking observed in single-unit recordings. These findings, along with an extensive body of evidence, support the thesis that the inhibition of saccade-related neurons in the FEF is crucial for suppressing the prepotent prosaccade during antisaccade trials (Munoz and Everling, 2004). In a prior study of response monitoring that examined the neural sequelae of error vs. correct antisaccade responses in ASD, we used the same paradigm and sample as the present study and reported a higher antisaccade error rate and faster latencies of correct antisaccades in ASD (Thakkar et al., 2008). In the present study, we tested the hypothesis that these behavioral inhibition deficits in ASD would be paralleled by reduced inhibition of the FEF as indexed by reduced fMRI activation for correct antisaccade vs. prosaccade trials.

Second, we examined the anterior cingulate cortex (ACC) based on its role in the top-down control of ocular motor regions, including the FEF (Johnston et al., 2007), and on evidence of functional and structural ACC abnormalities in ASD, including during response inhibition (Kana et al., 2007). Like the FEF, the ACC consistently shows greater activation for antisaccades vs. prosaccades in neuroimaging studies (e.g., Brown et al., 2006; Doricchi et al., 1997; Ford et al., 2005; Manoach et al., 2007; Matsuda et al., 2004; Paus et al., 1993). The posterior part of the dorsal ACC (dACC) has been labeled the “cingulate eye field” based on its involvement in tasks requiring volitional, but not reflexive saccadic control (Gaymard et al., 1998; Paus et al., 1993; Pierrot-Deseilligny et al., 2004) and because in monkeys, stimulation of this region evokes saccades (Mitz and Godschalk, 1989). In humans, lesions of the posterior dACC increase antisaccade errors (Milea et al., 2003) and prolong the latencies of both prosaccades and antisaccades (Gaymard et al., 1998). In ASD, there is growing evidence of both functional and structural abnormalities of the ACC. ASD samples show abnormal ACC activation during a range of cognitive tasks (Ashwin et al., 2007; Dichter and Belger, 2007; Gomot et al., 2006; Hall et al., 2003; Haznedar et al., 1997, 2000; Kennedy et al., 2006; Silk et al., 2006), including reduced ACC activation and reduced functional connectivity of the ACC during manual response inhibition (Kana et al., 2007). Consistent with a prior report (Barnea-Goraly et al., 2004), we previously reported decreased microstructural integrity of the white matter underlying the ACC in the present sample of individuals with ASD (Thakkar et al., 2008). These findings suggest aberrant functional and structural connectivity of the ACC in ASD, which might alter communication with other regions.

The ACC is structurally (Huerta et al., 1987; Morecraft et al., 1993; Pandya et al., 1981; Wang et al., 2004) and functionally (Koski and

Paus, 2000; Margulies et al., 2007) connected to premotor, motor, and ocular motor regions, including the FEF, consistent with its putative role in providing top-down control of structures generating motor (Miller and Cohen, 2001) and ocular motor (Johnston et al., 2007) responses. Single-neuron recordings in monkeys performing prosaccades and antisaccades show that the ACC is recruited during task preparation when cognitive demands increase, consistent with a role in top-down control of ocular motor structures (Johnston et al., 2007). These findings led us to theorize that during preparation to perform an antisaccade vs. a prosaccade, the dACC coordinates with the FEF to increase inhibitory control.

In the present study we predicted that ASD participants would show reduced activation of the dACC during antisaccades vs. prosaccades, reflecting reduced cognitive control. We also tested the hypothesis that ASD participants would show reduced coordination of activity in the dACC and FEF during saccadic performance by conducting a functional connectivity analysis of our fMRI data using seed regions in the right and left dACC. Functional connectivity MRI (Biswal et al., 1995) has proven to be a powerful method for evaluating network dysfunction in neuropsychiatric disorders (for review see, Buckner et al., 2008; Cherkassky et al., 2006; Kennedy and Courchesne, 2008; e.g., Kleinhans et al., 2008) and there is compelling evidence for the “underconnectivity” theory of autism, which posits that reduced coordination of activity across brain regions gives rise to symptoms and cognitive deficits (Just et al., 2004).

In summary, we hypothesized that deficient saccadic inhibition in ASD compared to healthy participants would be paralleled by decreased activation of the dACC and FEF during antisaccade vs. prosaccade trials reflecting reduced cognitive control in response to a cue that indicates a task with increased cognitive demand. Second, we hypothesized that there would be reduced functional connectivity between the dACC and FEF during saccadic performance in ASD reflecting reduced coordination of activity between these regions, which could also compromise inhibitory control. Finally, we examined whether FEF and dACC activation and functional connectivity were associated with RRB in ASD, since deficits in inhibiting prepotent responses may contribute to difficulty in flexibly adjusting responses based on context.

## Methods

### Participants

Eleven adults with ASD and 14 healthy control (HC) participants were recruited by poster and website advertisements. Participants with ASD were diagnosed with high functioning autism ( $n=7$ ), Asperger's disorder ( $n=2$ ), or pervasive developmental disorder, not otherwise specified ( $n=2$ ) by an experienced clinician (RMJ) on the basis of current presentation and developmental history as determined by medical record review and clinical interview. Potential participants meeting DSM-IV criteria for co-morbid psychiatric conditions or substance abuse were excluded. ASD diagnoses were confirmed using the Autism Diagnostic Interview-Revised (ADI-R, Rutter et al., 2003) and the Autism Diagnostic Observation Schedule Module 4 (Lord et al., 1999) administered by trained and experienced research personnel with established reliability. Individuals with known autism-related medical conditions (e.g., Fragile-X syndrome, tuberous sclerosis) were not included. Four of the 11 ASD participants were taking the following medications: fluoxetine and lithium; bupropion and clonazepam; citalopram; and sertraline and methylphenidate.

Healthy control participants were screened to exclude a history of autism or any other neurological or psychiatric condition (SCID-Non-patient edition, First et al., 2002). All participants were screened to exclude substance abuse or dependence within the preceding six months, and any independent condition that might affect brain

**Table 1**

Means, standard deviations, and group comparisons of demographic data. The Phi value is the result of a Fisher's Exact Test. The z value is the result of a nonparametric Mann-Whitney U comparison.

Subject characteristics	Healthy controls (n = 14)	ASD (n = 11)	t	p
Age	27 ± 8	28 ± 10	-0.30	0.77
Sex	8M/6F	9M/2F	$\phi = 0.26$	0.23
Laterality score (handedness)	75 ± 45	63 ± 37	0.73	0.47
Parental SES <sup>a</sup>	1.31 ± 0.48	1.18 ± 0.40	$z = 0.59$	0.43
Years of education	16 ± 2	16 ± 4	-0.32	0.75
Estimated verbal IQ	114 ± 9	117 ± 8	-0.96	0.35

<sup>a</sup> A lower score denotes higher status.

function. ASD and control groups were matched for age, sex, handedness as measured by a laterality score on the modified Edinburgh Handedness Inventory (scores of -100 and +100 denote exclusive use of left or right hands, respectively, Oldfield, 1971; White and Ashton, 1976), parental socioeconomic status on the Hollingshead Index (Hollingshead, 1965), years of education, and estimated verbal IQ based on a test of single word reading (American National Adult Reading Test, Blair and Spreen, 1989) (Table 1). All ASD participants had average or above estimates of verbal ( $124 \pm 12$ , range: 106 - 141) and nonverbal ( $120 \pm 10$ , range: 100 - 138) IQ as measured by the Wechsler Abbreviated Scale of Intelligence (Wechsler, 1999). The study was approved by the Partners Human Research Committee. All participants gave written informed consent after the experimental procedures had

been fully explained. One ASD participant was excluded from the event-related fMRI analysis due to technical problems with eye tracking that made it impossible to reliably classify erroneous vs. correct saccadic responses, but was included in the functional connectivity analyses, which examines correlations in activation across the entire fMRI time course.

*Saccadic paradigm*

Fig. 1 provides a graphic depiction of the task and a description of task parameters. Prior to scanning, the task was explained and participants practiced in a mock scanner until their performance indicated that they understood the directions and were comfortable with the task. Participants were instructed to respond as quickly and accurately as possible and told that they would receive a 5-cent bonus for each correct response in addition to a base rate of pay. This incentive was intended to enhance motivation and attention during a potentially boring cognitive task in order to elicit optimal performance. No immediate feedback regarding performance was provided and the bonus was added to the remuneration check, which was sent by mail following study completion. Each run of the task consisted of a pseudorandom sequence of prosaccade and antisaccade trials that were balanced for right and left movements. Randomly interleaved with the saccadic trials were intervals of fixation lasting 2, 4, or 6 s. The fixation intervals provided a baseline and their variable length introduced "temporal jitter," which optimizes the analysis of rapid

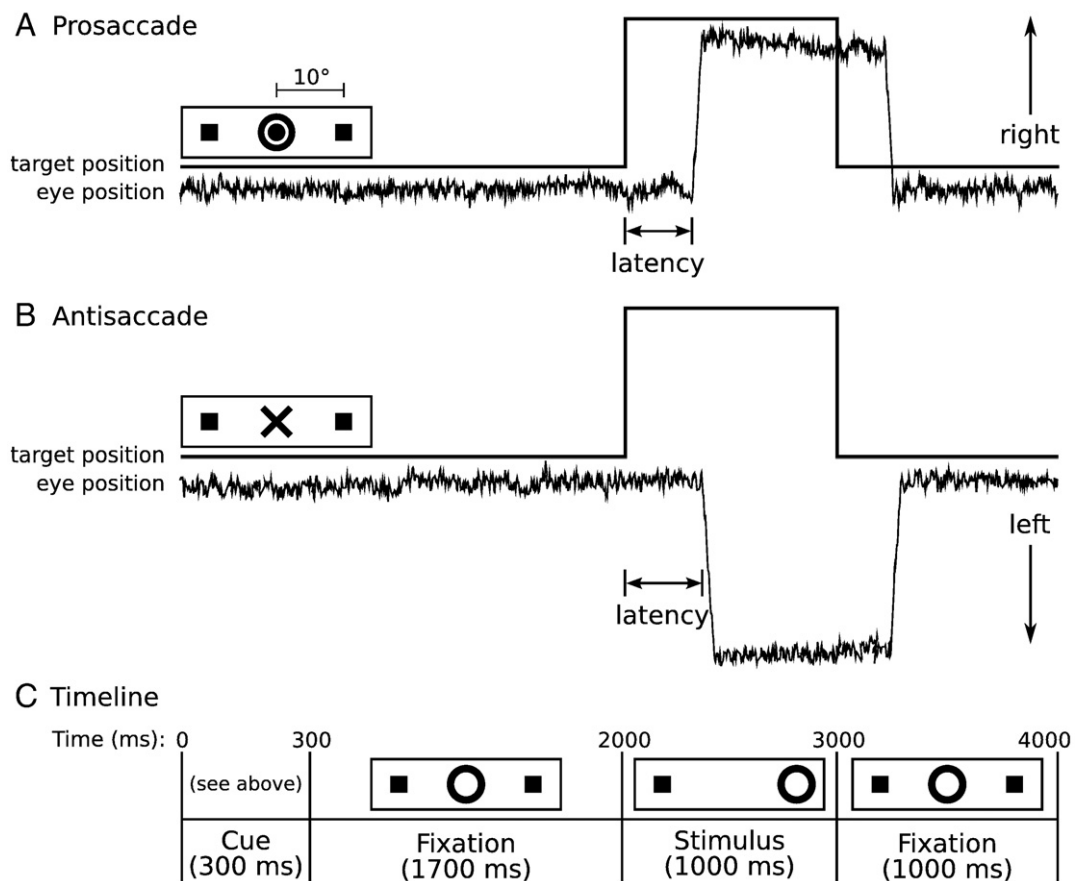


**Fig. 1.** Saccadic paradigm with idealized eye position traces. Saccadic trials lasted 4000 ms and began with an instructional cue at the center of the screen. For half of the participants, orange concentric rings were the cue for a prosaccade trial (A) and a blue X was the cue for an antisaccade trial (B). These cues were reversed for the rest of the participants. The cue was flanked horizontally by two small green squares of 0.2° width that marked the potential locations of stimulus appearance, 10° left and right of center. These squares remained on the screen for the duration of each run. C: At 300 ms, the instructional cue was replaced by a green fixation ring at the center of the screen, of 0.4° diameter and luminance of 20 cd/m<sup>2</sup>. After 1700 ms, the ring shifted to one of the two target locations, right or left, with equal probability. This was the stimulus to which the participant responded by either making a saccade to it (prosaccade) or to the square on the opposite side (antisaccade). The green ring remained in the peripheral location for 1000 ms and then returned to the center, where participants were also to return their gaze for 1000 ms before the start of the next trial. Fixation intervals were simply a continuation of the fixation display that constituted the final second of the previous saccadic trial.

presentation event-related fMRI designs (Buckner et al., 1998; Burock and Dale, 2000; Miezin et al., 2000). The schedule of events was determined using a technique to optimize the statistical efficiency of event-related designs (Dale, 1999). Participants performed six runs of the task, each lasting 5 min 22 s, with short rests between runs. The total experiment lasted about 40 min and generated a total of 211 prosaccade and 211 antisaccade trials, and 80 fixation intervals.

#### Stimulus display and eye tracking

Displays of the eye movement task were generated using the Vision Shell programming platform ([www.visionshell.com](http://www.visionshell.com)), and back-projected with a Sharp XG-2000 color LCD projector (Osaka, Japan) onto a screen at the rear of the bore that was viewed by the participant via a mirror on the head coil. The ISCAN fMRI Remote Eye Tracking Laboratory (ISCAN, Burlington, MA) recorded saccades during scanning. This system used a video camera mounted at the rear of the MRI bore. The camera imaged the eye of the participant via an optical combiner, a 45° cold transmissive mirror that reflects an infrared image of the eye, with the infrared illumination being provided by an LED mounted on the head coil. The system used passive optical components with no ferrous content within the bore to minimize artifacts in the MRI images. Eye position was sampled at a rate of 60 Hz. Eye images were processed by ISCAN's RK-726PCI high resolution Pupil/Corneal reflection tracker, located outside of the shielded MRI room. Stimuli presented by Vision Shell were digitally encoded and relayed to ISCAN as triggers that were inserted into the eye-movement recordings.

#### Scoring and analysis of eye movement data

Eye movement data were scored in MATLAB (Mathworks, Natick, MA) using a partially automated program that determined the directional accuracy of each saccade with respect to the required response and the latency from target onset. Saccades were identified as horizontal eye movements with velocities exceeding 47 deg/s. The onset of a saccade was defined as the point at which the velocity of the eye movement first exceeded 31 deg/s. Only trials with saccades in the desired direction and latencies over 130 ms were considered correct, and only correct saccades were included in the latency analyses. The cutoff of 130 ms excluded anticipatory saccades, which are executed too quickly to be a valid response to the appearance of the target (Fischer and Breitmeyer, 1987).

#### Image acquisition

Images were acquired with a 3.0T Siemens Trio whole body high-speed imaging device equipped for echo planar imaging (EPI) (Siemens Medical Systems, Erlangen, Germany). Head stabilization was achieved with cushioning, and all participants wore earplugs (29 dB rating) to attenuate noise. Automated shimming procedures were performed and scout images were obtained. Two high-resolution structural images were acquired in the sagittal plane for slice prescription, spatial normalization (spherical and Talairach), and cortical surface reconstruction using a high resolution 3D magnetization prepared rapid gradient echo (MPRAGE) sequence (repetition time (TR), 2530 ms; echo spacing, 7.25 ms; echo time (TE), 3 ms; flip angle 7°) with an in-plane resolution of 1 mm and 1.3 mm slice thickness. T1 and T2-weighted structural images, with the same slice specifications as the Blood Oxygen Level Dependent (BOLD) scans, were obtained to assist in registering functional and structural images. Functional images were collected using a gradient echo T2\* weighted sequence (TR/TE/Flip = 2000 ms/30 ms/90°). Twenty contiguous horizontal slices parallel to the intercommissural plane (voxel size: 3.13 × 3.13 × 5 mm) were acquired interleaved. The functional sequences included prospective acquisition correction (PACE) for

head motion (Thesen et al., 2000). PACE adjusts slice position and orientation in real time during data acquisition. This reduces motion-induced effects on magnetization history.

#### Surface-based fMRI analyses

In addition to on-line motion correction (PACE), functional scans were corrected retrospectively for motion using the AFNI algorithm (Cox and Jesmanowicz, 1999). To characterize average motion for each participant, total motion in mm for all six directions (*x*, *y*, *z*, and three rotational directions) as determined by AFNI, was averaged across the six runs of the task and compared between groups. All further analyses were conducted using FreeSurfer (<http://surfer.nmr.mgh.harvard.edu>) and FreeSurfer Functional Analysis Stream (FS-FAST) software. Following motion correction, scans were intensity normalized, and smoothed using a 3D 8 mm FWHM Gaussian kernel. Finite impulse response (FIR) estimates (Burock and Dale, 2000; Miezin et al., 2000) of the event-related hemodynamic responses were calculated for each of the three trial types (correct prosaccades, correct antisaccades, and errors) for each participant. This involved using a linear model to provide unbiased estimates of the average signal intensity at each time point for each trial type without making *a priori* assumptions about the shape of the hemodynamic response. Hemodynamic response estimates were computed at 12 time points with an interval of 2 s (corresponding to the TR) ranging from 4 s prior to the start of a trial to 18 s after the start. Temporal correlations in the noise were accounted for by prewhitening using a global estimate of the residual error autocorrelation function truncated at 30 s (Burock and Dale, 2000).

Functional volumes were aligned to the 3D structural image for each participant, which was created by averaging the two MPRAGE scans after correcting for motion. The averaged MPRAGE scans were used to construct inflated (2D) models of individual cortical surfaces using previously described segmentation, surface reconstruction, and inflation algorithms (Dale et al., 1999; Fischl et al., 1999a). To register data across participants, anatomical and functional scans were spatially normalized using a surface-based spherical coordinate system that explicitly aligns cortical folding patterns (Dale et al., 1999; Fischl et al., 1999a,b). Registered group data were smoothed with a 2D 4.6 mm FWHM Gaussian kernel.

fMRI results were displayed on a template brain consisting of the averaged cortical surface of an independent sample of 40 adults from the Buckner laboratory at Washington University. To facilitate comparison with other studies, approximate Talairach coordinates were derived by mapping the surface-based coordinates of activation back to the original structural volume for each participant, registering the volumes to the Montreal Neurological Institute (MNI305) atlas (Collins et al., 1994) and averaging the MNI305 coordinates that corresponded to the surface maxima across participants. The resulting coordinates were transformed to standard Talairach space using an algorithm developed by Matthew Brett (<http://imaging.mrc-cbu.cam.ac.uk/imaging/MniTalairach>).

#### Regions of Interest (ROI) definitions

The FEF was defined using a combination of anatomical constraints and activation in a contrast orthogonal to our contrast of interest, antisaccade vs. prosaccade trials. We anatomically defined the FEF as vertices in and around the precentral sulcus and gyrus, beginning approximately at the level of the superior frontal sulcus (Koyama et al., 2004; Paus, 1996). The medial hemispheric surface was not included. Within this area, we defined the ROI as all active vertices in the contrast of all saccades versus fixation at 4 s (the time of peak activity in ocular motor regions) at a threshold of  $p < 0.001$  in the averaged data of all participants. This contrast captures task-related activity and is unbiased to differences between groups or trial types. This process resulted in two FEF labels, one in each hemisphere.

The dACC was localized using a parcellation algorithm that provides labels for ACC (Fischl et al., 2004). The ACC labels were divided into dorsal and rostral segments by drawing a line perpendicular to the intercommissural plane at the anterior boundary of the genu of the corpus callosum (Devinsky et al., 1995) resulting in left and right dACC labels. We did not use a functional constraint, since we found only weak activation in the contrast of all saccades vs. fixation in the combined group. This is not surprising given the literature, reviewed above, which finds that dACC is more strongly recruited on tasks with high cognitive demands and consistently shows greater fMRI activation for antisaccades vs. prosaccades.

#### Vertex-wise analysis of the cortical surface

Our primary analysis was a group comparison of activation for the contrast of correct antisaccade and prosaccade trials at 4 s following the trial onset (i.e., “inhibition-related activation”) at each vertex using a random effects model. We also examined group differences in each condition (antisaccades and prosaccades) compared to the fixation baseline. To correct for multiple comparisons we ran 5000 Monte Carlo simulations of synthesized white Gaussian noise using a  $p$ -value of  $\leq 0.05$  and the smoothing, resampling, and averaging parameters of the functional analysis. This determines the likelihood that a cluster of a certain size would be found by chance for a given threshold. To test our *a priori* hypotheses concerning the FEF and dACC, we restricted the simulations to the FEF and dACC ROIs. To explore whether other regions also showed significant group differences we also ran simulations on the entire cortical surface.

#### Regressions of activation on behavioral and clinical measures

To examine the relations of inhibition-related activation in our ROIs with antisaccade performance, both error rate and the latency of correct responses, we performed linear regressions. An interaction term with group (e.g., error rate by group) was included in the model to determine whether the slope of the relations differed by group. We also regressed inhibition-related activation on ADI-R diagnostic algorithm scores of RRB for the ASD group only.

#### Volume-based functional connectivity analysis

##### Preprocessing

The motion-corrected functional scans were registered to the Montreal Neurological Institute (MNI152) atlas (Collins et al., 1994) using FSL (FMRIB Software Library, [www.fmrib.ox.ac.uk/fsl](http://www.fmrib.ox.ac.uk/fsl)). Additional preprocessing steps, described in previous reports (Fox et al., 2005; Van Dijk et al., in press; Vincent et al., 2006), were: 1) spatial smoothing using a Gaussian kernel of 6 mm full-width at half-maximum; 2) temporal filtering ( $0.009 \text{ Hz} < f < 0.08 \text{ Hz}$ ); 3) removal of spurious or nonspecific sources of variance by regression of the following variables: (a) the six movement parameters computed by rigid body translation and rotation in preprocessing, (b) the mean whole brain signal, (c) the mean signal within the lateral ventricles, and (d) the mean signal within a deep white matter ROI. The first temporal derivatives of these regressors were included in the linear model to account for the time-shifted versions of spurious variance. Regression of each of these signals was computed simultaneously and the residual time course was retained for the correlation analysis.

##### Definition of dACC seed regions and FEF ROIs

We defined dACC seed regions using fMRI activation constrained by MNI anatomical criteria for the ACC. In the averaged functional data of all participants, we identified voxels in the left and right dACC that showed inhibition-related fMRI activation at a threshold of  $p < 0.05$ . We defined FEF ROIs based on anatomical criteria, as described above, and voxels that showed inhibition-related fMRI activation at a threshold of  $p < 0.001$  in the averaged functional data of all participants.

#### Data analysis

BOLD time courses of the right and left dACC seed regions were based on the average signal across voxels. A Pearson correlation map was created for the time course of each seed region and of all the other voxels in the brain. The correlation map of each individual was converted to a map of  $z$ -scores using a Fisher's  $z$  transform (see, Vincent et al., 2006). We first examined functional connectivity of the dACC with the FEF in each group separately. We then compared functional connectivity by group using  $t$ -tests. We ran 5000 Monte Carlo simulations, restricted to the right and left FEFs, to correct for multiple comparisons. These simulations used a  $p$ -value of  $\leq 0.05$  and the smoothing, resampling, and averaging parameters of the functional connectivity analysis.

## Results

### Saccadic performance

As previously reported (Thakkar et al., 2008), ASD participants made significantly more errors than healthy controls ( $F(1,22) = 7.82$ ,  $p = 0.008$ ). Although the group by task interaction was not significant ( $F(1,22) = 0.99$ ,  $p = 0.32$ ), ASD participants had a significantly higher antisaccade error rate than controls (Fig. 2A,  $t(22) = 2.68$ ,  $p = 0.01$ , HC:  $6.55 \pm 4.94\%$ , range 1.43 to 16.59%; ASD:  $12.41 \pm 9.02\%$ , range 2.37 to 26.67%), but did not differ significantly in the error rate for prosaccades (Fig. 2A,  $t(22) = 1.62$ ,  $p = 0.21$ , HC:  $2.04 \pm 1.50\%$ , ASD:  $4.82 \pm 4.06\%$ ). ASD participants responded more quickly on correct trials ( $F(1,21) = 9.74$ ,  $p = 0.005$ ) and there was a trend to a group by task interaction ( $F(1,21) = 3.33$ ,  $p = 0.08$ ) reflecting a greater group latency difference for antisaccade than prosaccade trials (Fig. 2B, antisaccade:  $t(21) = 3.47$ ,  $p = 0.002$ , HC:  $309 \pm 40$  ms, ASD:  $253 \pm 20$  ms; prosaccade:  $t(21) = 2.56$ ,  $p = 0.02$ , HC:  $254 \pm 50$  ms, ASD:  $212 \pm 29$  ms). In ASD, neither antisaccade error rate, nor latency of correct antisaccades showed significant correlations with ADI-R RRB scores (error rate:  $r = -0.26$ ,  $p = 0.46$ ; latency:  $r = -0.19$ ,  $p = 0.60$ ).

### Surface-based analyses of activation in ROIs

The results of the exploratory analyses of the entire cortical surface are presented as supplemental material.

### Group comparisons

ASD participants and controls did not differ in mean motion during the functional scans (controls:  $1.71 \pm 0.81$  mm, patients:  $1.78 \pm$

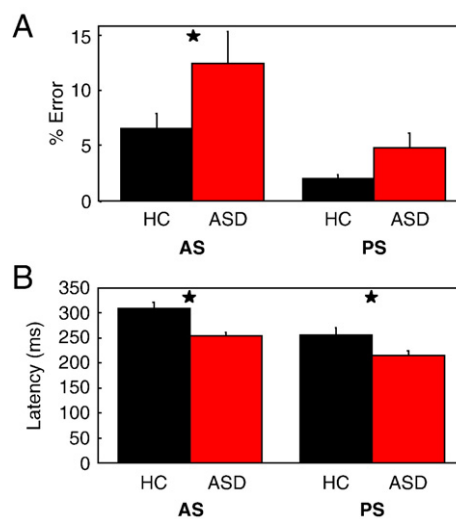
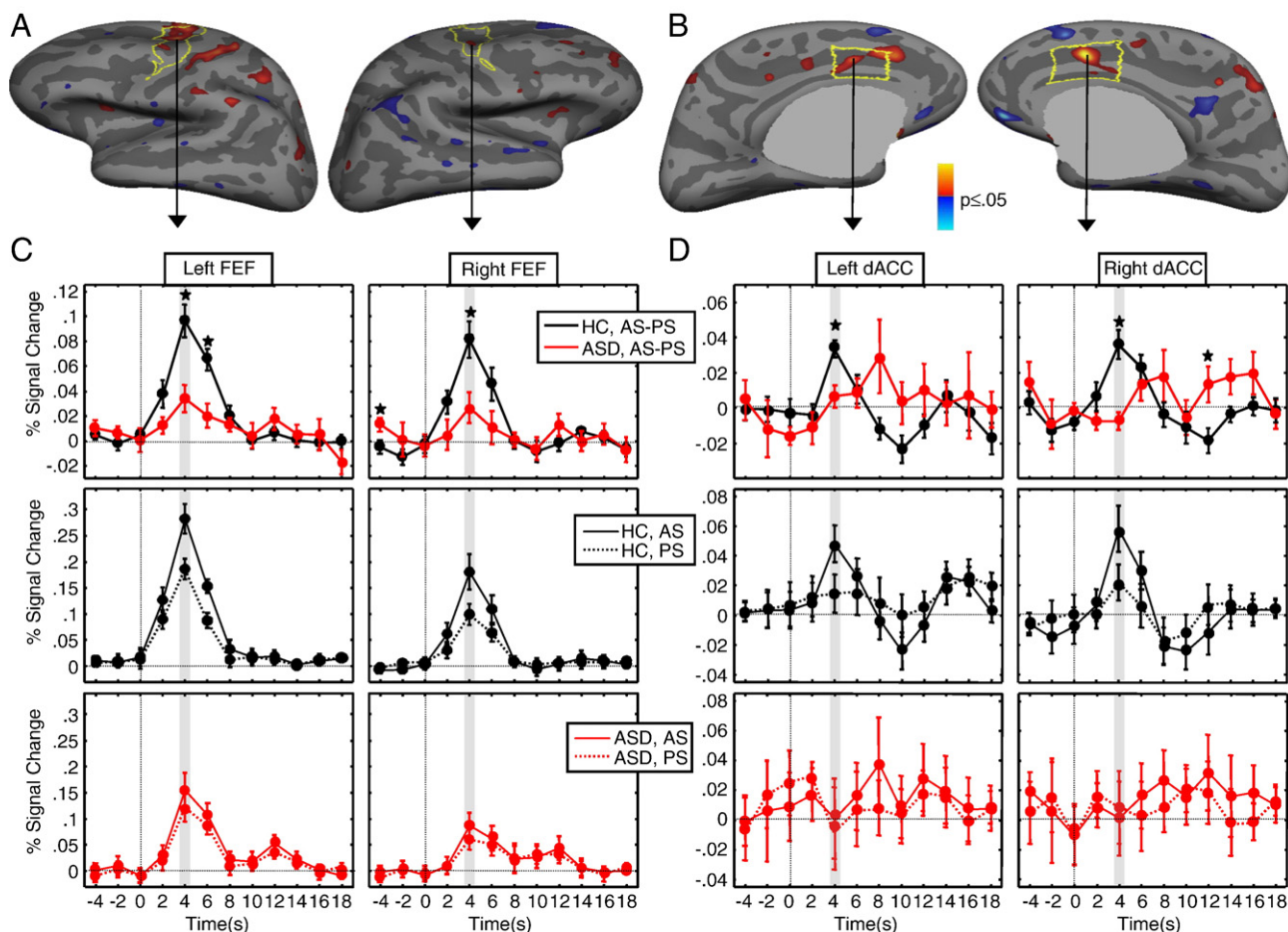


Fig. 2. Behavioral results for the control and ASD groups. (A) Antisaccade error rate. (B) Latency of correct antisaccades and correct prosaccades. Asterisks denote statistical significance of group difference at  $p \leq 0.05$ .



**Fig. 3.** Frontal eye field (FEF) and dorsal anterior cingulate (dACC) activation. (A, B) Statistical maps of group differences in fMRI activation at 4 s for the antisaccade versus prosaccade contrast. Statistical maps are displayed on the inflated cortical surfaces of the template brain at  $p < 0.05$ . Regions of greater activation in controls are depicted in warm colors; greater activation in ASD patients is depicted in blue. The regions of interest are outlined in yellow. The gray masks cover subcortical regions in which activity is displaced in a surface rendering. (C, D) Hemodynamic response functions. All plots correspond to the vertex that showed the largest contrast effects within the respective ROI. The top row shows activation in antisaccade versus prosaccade trials. The middle and bottom rows show activation for the control and ASD groups, respectively, during antisaccade and prosaccade trials separately, each relative to the fixation condition. Asterisks denote significance levels of  $p \leq 0.05$  at individual time points.

0.47 mm,  $t(22) = 0.62$ ,  $p = 0.83$ ). Relative to controls, ASD participants showed significantly reduced inhibition-related activation in bilateral FEF and dACC (Fig. 3, see Table 2 for cluster-wise probabilities). To visualize the source of these differences, we plotted the hemodynamic responses of inhibition-related activation for both the group comparison and for each group separately. Inspection of these plots confirmed that in bilateral FEF and dACC, the greater difference in inhibition-related activation for controls compared to ASD participants was due to a greater increase in positive activation for antisaccades compared to prosaccades. A comparison of group differences in each condition (antisaccades and prosaccades) compared to the fixation baseline revealed that ASD participants showed significantly reduced activation in left FEF (CWP = 0.0001) and bilateral dACC (left: CWP = 0.04, right: CWP = 0.0002) for antisaccades and in left FEF for prosaccades (CWP = 0.04).

#### Relation of inhibition-related activation to antisaccade performance

Greater inhibition-related activation in right dACC predicted a lower antisaccade error rate for the combined group (Fig. 4A, Table 2), and in each group separately, and this relation did not differ significantly by group. Activation in the other ROIs did not significantly predict error rate, and there were no significant group differences. With regard to the latency of correct antisaccades, there were no significant relations with activation in the combined group. There was a group difference, however, in the left dACC (Table 2). While controls showed no significant relations between

activation and latency, in ASD participants, greater inhibition-related activation in both the left and right dACC predicted faster antisaccades (Fig. 4B).

#### Relation of inhibition-related activation to restricted, repetitive behavior in ASD

Greater left FEF activation predicted increased severity of RRB in ASD (Fig. 4C, Table 2).

#### Volume-based functional connectivity analysis

Both the right and left dACC seeds were significantly positively correlated with right and left FEF in both groups. As predicted, controls showed significantly stronger correlations of both dACC seeds with the left FEF (Fig. 5, Table 3). Functional connectivity between dACC and FEF was not related to either antisaccade error rate or latency in the combined group, and there were no group differences in these relations. In participants with ASD, we examined whether abnormally reduced dACC-FEF functional connectivity, which was quantified by averaging across FEF voxels in the cluster showing a significant group difference ( $p < 0.05$ ), correlated with RRB. Both the left and right dACC showed a positive relation with RRB (i.e., greater functional connectivity predicted more severe RRB), but this was only significant for left dACC (left:  $r = 0.64$ ,  $p = 0.03$ ; right:  $r = 0.37$ ,  $p = 0.27$ ).

**Table 2**  
Maxima and locations of cluster, antisaccade vs. prosaccade contrast within the FEF and dACC ROIs.

Cortical region of interest	Cluster size (mm <sup>2</sup> )	Direction of difference	Approximate Talairach coordinates			Brodmann area	t-value (max)	CWP
			x	y	z			
<i>Inhibition-related activation</i>								
Left FEF <sup>a</sup>	364	HC>ASD	-25	-7	43	6	3.06	0.0002
Left dACC	268	HC>ASD	-11	20	26	32	3.27	0.003
Right dACC	299	HC>ASD	11	21	26	62	4.19	0.0005
Right FEF	194	HC>ASD	27	-2	42	24	2.58	0.002
<i>Relations with antisaccade error rate</i>								
Combined group								
Right dACC	206	r<0	4	15	31	24	-2.44	0.001
Control group								
Right dACC	162	r<0	12	23	24	32	-2.31	0.003
ASD group								
Right dACC	136	r<0	8	20	32	32	-2.69	0.005
<i>Relations with antisaccade latency</i>								
Group difference in slope								
Left dACC	355	HC>ASD	-2	8	26	24	3.81	0.0002
ASD group								
Left dACC	369	r<0	-3	13	23	24	-2.64	0.0002
Right dACC	133	r<0	4	1	27	24	-3.61	0.005
<i>Relations with ADI-R RBB scores, ASD group</i>								
Left FEF	98	r>0	-25	-6	44	6	3.80	0.04
Left FEF <sup>a</sup>	320	r>0	-41	1	27	6	3.56	0.0002

<sup>a</sup> Also meets correction for entire cortical surface.

#### Control analyses: medication effects

Excluding ASD participants on psychotropic medications presents both pragmatic and interpretive difficulties. In current practice, adults with ASD, even those without co-morbid psychiatric disorders, are frequently medicated. Thus, excluding medicated patients not only makes it difficult to recruit participants in a medical setting, but might also compromise the generalizability of the findings. In our prior behavioral study, medication status did not affect the directional accuracy or latency of either prosaccades or antisaccades in ASD (Manoach et al., 2004). In the present study, four of our ASD participants were taking a variety of medications. A scatter plot of inhibition-related activation in each of our four ROIs (Fig. 6), however, indicates that the medicated ASD participants did not disproportionately contribute to the group difference. Medicated ASD patients did not differ from unmedicated patients in inhibition-related activation in either FEF ROI or in the right dACC, but showed increased activation in left dACC ( $t(8) = 2.86$ ,  $p = 0.02$ , uncorrected for multiple comparisons), which served to reduce the difference between ASD and control participants. In addition, comparisons of medicated and unmedicated ASD participants on our behavioral (saccadic directional accuracy and latency) and functional connectivity (right and left dACC seed regions) outcome measures, did not reveal any significant differences.

#### Discussion

The present study demonstrates functional abnormalities in two anatomical components of the network serving volitional ocular motor control in ASD that may contribute to deficient saccadic inhibition and to rigid, inflexible behavior. Compared to controls, ASD participants made more antisaccade errors and showed reduced inhibition-related activation (based on the contrast of correct antisaccades vs. prosaccades) in bilateral FEF and dACC during correct trials. Moreover, reduced dACC activation correlated with a higher error rate in both groups and longer antisaccade latencies in ASD.

Given that the ACC is thought implement top-down control of the FEF (Johnston et al., 2007) and that lesions of the dACC increase antisaccade errors and prolong saccadic latencies (Gaymard et al., 1998; Milea et al., 2003), these findings suggest that dACC activation reflects the implementation of cognitive control over behavior, and that this control is compromised in ASD.

Decreased functional connectivity between the dACC and FEF may contribute to compromised cognitive control over behavior in ASD. The ACC is reciprocally connected to the FEF in monkeys (Huerta et al., 1987; Morecraft et al., 1993; Pandya et al., 1981; Wang et al., 2004). Consistent with a prior fMRI resting state study of humans (Margulies et al., 2007), we found strong positive correlations between activation in the dACC and FEF in both controls and ASD participants during saccadic performance. In ASD, however, the strength of these correlations was significantly reduced. These findings are consistent with the hypothesis that during preparation to perform an antisaccade vs. a prosaccade, the dACC coordinates with the FEF to increase inhibitory control and that this interaction is disrupted in ASD. This disruption may contribute to the consistently observed deficit in saccadic inhibition in ASD (Goldberg et al., 2002; Luna et al., 2007; Manoach et al., 2004, 1997; Minshew et al., 1999; Mosconi et al., 2009; Thakkar et al., 2008). The present finding of reduced dACC functional connectivity with FEF in ASD complements our prior report of decreased microstructural integrity of the white matter underlying the ACC in the same sample (Thakkar et al., 2008) and suggests that functional and structural ACC abnormalities compromise the cognitive control of behavior in ASD.

Based on a prior report showing that a behavioral measure of response inhibition (i.e., antisaccade error rate) correlated with greater severity of RRB in ASD (a finding we did not replicate here, Mosconi et al., 2009), we investigated whether the neural correlates of response inhibition were also related to RRB. We reasoned that since the inhibition of prepotent but contextually inappropriate behaviors is essential to adaptive, flexible responding, activation during response inhibition might be associated with the severity of RRB in ASD. We found that greater inhibition-related activation in left FEF correlated with more severe RRB. In interpreting this finding, we note that antisaccade error rate and inhibition-related fMRI activation, which is based on the comparison of correct antisaccades vs. prosaccades, are not directly comparable. While errors reflect a failure of response inhibition, inhibition-related activation reflects the magnitude of difference in activation between antisaccades and prosaccades required for successful response inhibition. Thus, our findings suggest that within the ASD group, individuals with more severe behavioral rigidity and repetition required a higher level of activation in the FEF to successfully inhibit a prepotent response. The relation of greater functional connectivity of dACC to FEF with more severe RRB suggests that greater inter-regional coordination was also required. As we did not find significant relations between dACC activation and RRB, the questions of whether deficient cognitive control over behavior contributes to RRB and whether increased FEF activation represents an attempt to compensate for decreased control remain unresolved.

These findings of relations of ACC function to a core feature of ASD add to a literature that documents relations between ACC function and social impairment (Haznedar et al., 2000; Henderson et al., 2006; Kennedy et al., 2006; Ohnishi et al., 2000), communication impairment (Haznedar et al., 2000; Ohnishi et al., 2000), and RRB (Shafritz et al., 2008). In these prior studies both increased and reduced ACC function were related to greater impairment in ASD. Similarly, there are reports of both decreased and increased ACC activation in ASD, using a variety of cognitive probes. Rather than reflecting discrepancies, these differences indicate that the direction of both group differences in activation and its relations with symptoms depend on a number of factors including the task employed, the specific time point examined, the cognitive process under study, and the ACC subregion

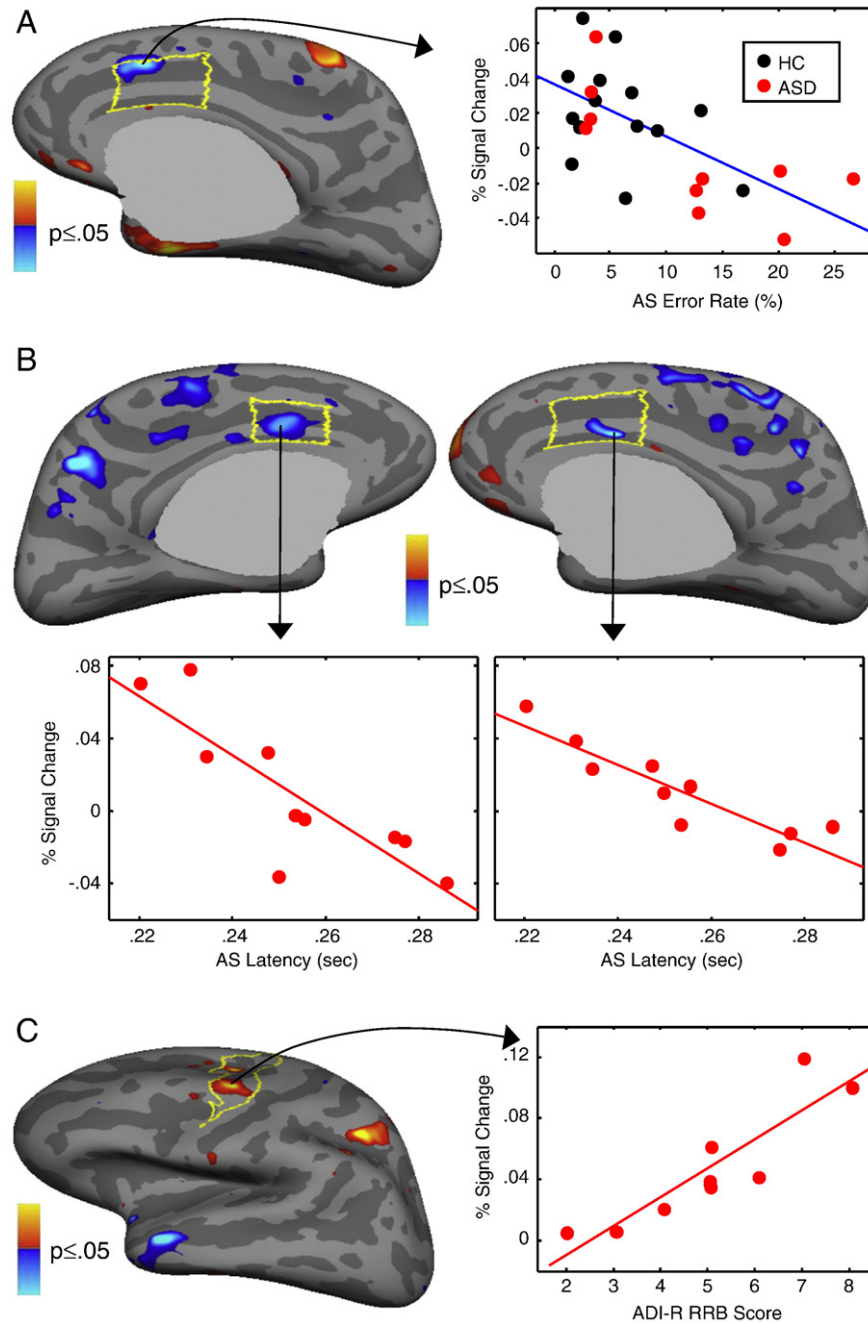


**Fig. 4.** Regressions of inhibition-related activation (i.e., antisaccade vs. prosaccade at 4 s) on behavioral and clinical measures. In all surface-based statistical maps, red and blue regions indicate positive and negative correlation, respectively. **A:** Antisaccade error rate in the combined group. The scatter plot shows activation in the vertex with the most significant correlation in the right dACC, which is outlined in yellow. **B:** Antisaccade latency in the ASD group. Scatter plots show activation in the most significant vertices in left and right dACC. **C:** ADI-R scores of RRB in the ASD group. Scatter plot shows activation in the vertex with the most significant correlation in the left FEF, outlined in yellow.

involved. For example, using the same saccadic paradigm as the present study in a neurotypical sample, we demonstrated both task-induced *deactivation* of a rostral ACC subregion early in correct antisaccade trials and *increased* activation of a different rostral ACC subregion later in the trial, following an error (Polli et al., 2005). Similarly, while in the present study, ASD participants showed abnormally reduced dACC activation for antisaccades early in correct trials, presumably reflecting deficient preparation, in our prior report, this same sample showed abnormally increased activation of a different dACC subregion following antisaccade errors, presumably reflecting hyperactive response monitoring (Thakkar et al., 2008). In both studies, increased dACC activation was related more severe RRB, consistent with the hypothesis that abnormalities in ACC-mediated

executive functions contribute to this multi-dimensional symptom cluster. This level of complexity (i.e., it is not a simple matter of more or less function) should be expected given the considerable heterogeneity of the ACC in terms of structure, function, and connectivity (Bush et al., 2000, 1998; Devinsky et al., 1995; Margulies et al., 2007; Phillips et al., 2003; Whalen et al., 1998) and the diverse paradigms and techniques used to probe its function. The present study was guided by regionally and temporally specific hypotheses that were based on our prior imaging and behavioral studies of this saccadic paradigm in both neurotypical and ASD participants (e.g., Manoach et al., 2007; Polli et al., 2005; Thakkar et al., 2008), an extensive literature concerning the functional neuroanatomy of saccadic inhibition (for review see Munoz and Everling, 2004), and a prior finding concerning the relation

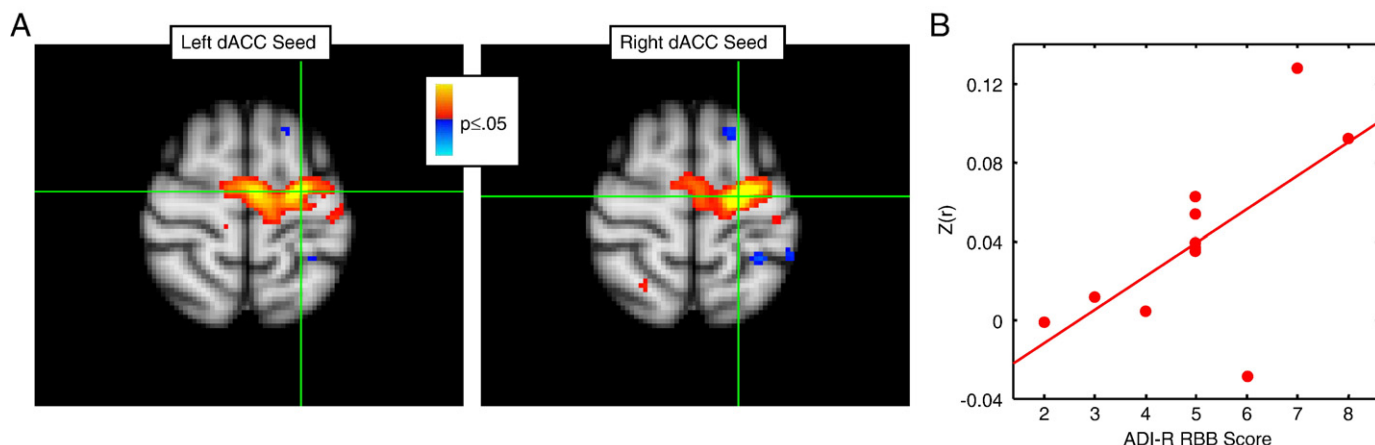


**Fig. 5.** Functional connectivity analysis. (A) Group differences in functional connectivity of the FEF. Red regions indicate stronger connectivity in controls. Green crosses indicate the location of the voxel that showed the strongest group difference for the respective seed region. (B) Regression against RRB in participants with ASD. The x axis indicates ADI-R scores of RRB, and the y axis indicates z-scores averaged across all FEF voxels that showed significant group differences in functional connectivity with the left dACC seed.

of saccadic inhibition deficits to RRB in ASD (Mosconi et al., 2009). Given our *a priori* hypotheses, the small sample, and concerns about multiple comparisons, we restricted our investigation to activation in the dACC and FEF and its relation to RRB.

There are now several neuroimaging studies of inhibition in ASD that employed manual response tasks. Using the Go–No–Go task, one study reported generally reduced activation compared to controls, primarily in the ACC and reduced functional connectivity of the ACC to middle cingulate gyrus and insula (Kana et al., 2007), consistent with the present findings. Another study of the Go–No–Go task reported increased activation in left ventrolateral prefrontal and orbitofrontal cortex in ASD (Schmitz et al., 2006). A recent study of the Preparing to Overcome Prepotency Task showed decreased prefrontal and parietal activation in adolescents with ASD and reduced frontoparietal functional connectivity (Solomon et al., 2009). In none of these studies did the ASD and control groups differ significantly in task performance.

More generally, behavioral evidence of deficient response inhibition in ASD is mixed, with both negative (e.g., Goldberg et al., 2005;

Kleinhans et al., 2005; Mahone et al., 2006; Ozonoff and Strayer, 1997) and positive findings (e.g., Bishop and Norbury, 2005; Geurts et al., 2004). Whether or not inhibition is intact in ASD likely depends both on the particular task and also on task-parameters, such as presentation rate (Raymaekers et al., 2004). Studies of antisaccades, in contrast, consistently find deficient inhibition in ASD, as indicated by a higher antisaccade error rate (Goldberg et al., 2002; Luna et al., 2007; Manoach et al., 2004, 1997; Minschew et al., 1999; Mosconi et al., 2009). This raises questions about why saccadic inhibition is so consistently disrupted in ASD and the possible clinical significance of this deficit. Antisaccades require a voluntary dissociation of spatial attention, which is compelled by the suddenly appearing stimulus, and eye gaze. Eye gaze and spatial attention are tightly linked (Corbetta and Shulman, 2002; Hunt and Kingstone, 2003; Klein and McCormick, 1989; Moore et al., 2003) and volitional control over both eye gaze and the spatial distribution of attention depend on a densely interconnected network with its key cortical components in the FEF, ACC and posterior parietal cortex, with the paralimbic ACC providing a map of motivational salience (Gitelman et al., 1999; Mesulam, 1981, 1990). Abnormalities in this circuitry may contribute to deficits in overcoming prepotency in the service of directing eye gaze and attention to the parts of the environment that are the most behaviorally relevant. Such a deficit could interfere with the development of social and cognitive skills that are deficient in ASD, including joint attention (Manoach et al., 1997; Mundy, 2003; Mundy et al., 2009).

It is important to note that because prosaccade and antisaccade trials are intermixed in our saccadic paradigm, both trial types require vigilance to instructional cues and volitional control. Therefore, both trial types rely on the volitional ocular motor control network that we hypothesize is deficient in ASD. In a prior study that compared single and mixed task blocks, prosaccade errors were only seen in the mixed-task blocks in both neurotypical participants and those with schizophrenia (Manoach et al., 2002). Thus, in the context of intermixed trials, prosaccade errors may reflect failures of proactive control (i.e., to adequately heed the instructional cue), which would likely have more pronounced effects on trials where greater control is needed (i.e., antisaccades more than prosaccades). In the present study, ASD participants performed prosaccades faster than controls, made numerically but not significantly more prosaccade errors, and showed significantly reduced left FEF activation in the contrast of prosaccades vs. fixation. Thus, while abnormalities in ASD were clearly more pronounced for antisaccades, prosaccades were also affected. Given the literature showing that visually guided saccades in ASD have normal latency

**Table 3**

Functional connectivity analyses: Maxima of FEF clusters showing significant positive functional connectivity with right and left dACC seeds and of FEF clusters showing significantly reduced positive functional connectivity in ASD.

Cortical region	Cluster size (mm <sup>3</sup> )	Approximate Talairach coordinates			Brodmann area	t-value (max)	CWP
		x	y	z			
<i>Left dACC seed</i>							
Control group							
Left FEF	6376	−18	−7	60	6	10.54	0.0002
Right FEF	7880	47	3	44	6	12.28	0.0002
ASD group							
Left FEF	6264	−44	−2	46	6	9.14	0.0002
Right FEF	5632	53	1	37	6	8.51	0.0002
<i>Right dACC seed</i>							
Control group							
Left FEF	6216	20	−3	59	6	12.95	0.0002
Right FEF	7568	34	−4	52	6	12.0	0.0002
ASD group							
Left FEF	4960	−22	2	52	6	9.93	0.0002
Right FEF	5544	53	1	37	6	7.81	0.0002
<i>Group difference (HC&gt;ASD)</i>							
Left dACC seed							
Left FEF	1728	−20	−15	62	6	3.82	0.03
Right dACC seed							
Left FEF	1592	−18	−9	60	6	5.52	0.04

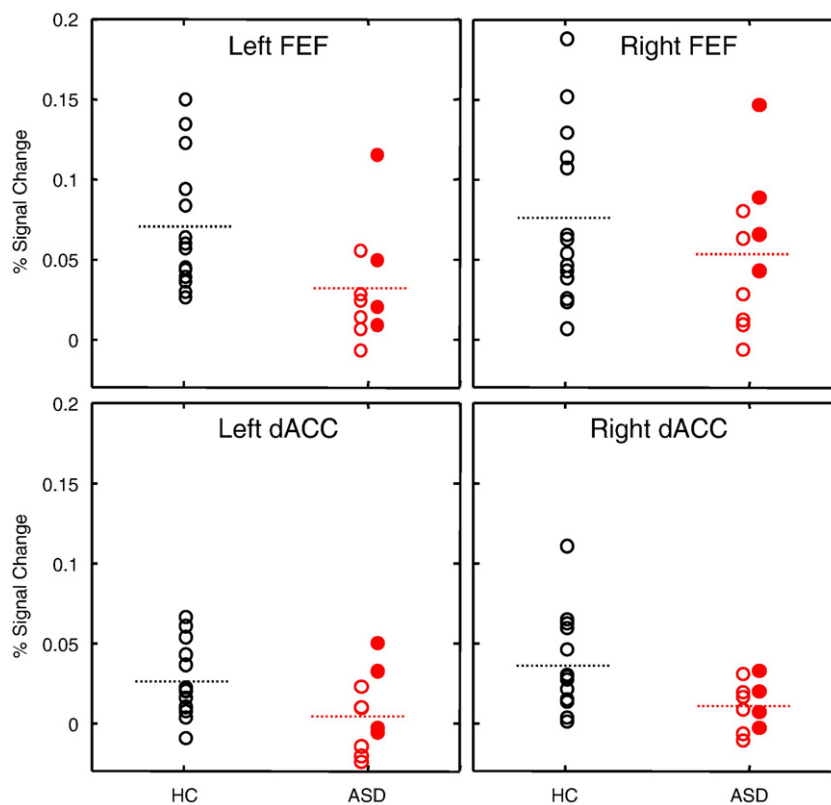


**Fig. 6.** The effect of medication on inhibition-related activation in participants with ASD. Each panel shows mean activation across all vertices in each of the four ROIs for the control and ASD groups. The control participants, none of whom were medicated, are indicated by open black circles. Within the ASD group, unmedicated participants are indicated by open red circles, and medicated participants are indicated by filled red circles. The dashed lines indicate group means (with all subjects included).

and directional accuracy (reviewed in, Rommelse et al., 2008), we attribute group differences in both trial types not to inhibition *per se*, but more generally to cognitive control, in this case ocular motor control, which is taxed to a greater degree by antisaccades than prosaccades. A limitation of the present study is that because we did not study reflexive saccades, we cannot rule out the possibility that abnormalities in the basic integrity of the ocular motor system in ASD contribute to our findings.

There are several other limitations to the present study that merit consideration. The first is that given the very small sample size, we consider our findings to be preliminary and to require replication in a larger sample. In spite of this, our *a priori* hypotheses concerning reduced inhibition-related activation in the dACC and FEF and reduced dACC-FEF functional connectivity were confirmed. A second issue is that four of our ASD participants were taking medications that affect brain function. Our comparisons of outcome measures in medicated and unmedicated ASD participants indicate that medicated participants did not contribute disproportionately to the group differences we observed (Fig. 6). Third, our sample was comprised of high functioning adults with ASD so it is not clear that our findings would generalize to lower functioning or younger samples. Although increased antisaccade error rates are seen in autism as early as ages 8 to 12 (Luna et al., 2007), we limited our study to adults since saccadic inhibition may not fully develop until late adolescence (Klein and Foerster, 2001) and larger samples would be necessary to discriminate between the effects of ASD and those due to normal development.

In summary, the present study represents the first neuroimaging investigation of the neural correlates of the saccadic inhibition deficit in ASD. In the context of an increased antisaccade error rate, ASD participants showed reduced inhibition-related activation in both the FEF and dACC, and reduced functional connectivity between these regions, complementing our prior report of reduced microstructural integrity of the white matter underlying the dACC in this ASD sample

(Thakkar et al., 2008). We interpret these findings to reflect that functional and structural dACC abnormalities compromise the voluntary control of spatial attention and eye gaze and contribute to deficits in overcoming prepotency in ASD. More generally, our findings are consistent with prior work in suggesting reduced cognitive control over behavior by the dACC in ASD (e.g., Solomon et al., 2009).

#### Acknowledgments

Funding: National Institute for Mental Health (R01 MH67720 (DSM); Mental Illness Neuroscience Discovery (MIND) Institute (DOE DE-FG02-99ER62764); The National Center for Research Resources (P41RR14075).

#### Appendix A. Supplementary data

Supplementary data associated with this article can be found, in the online version, at doi:10.1016/j.neuroimage.2010.04.010.

#### References

- Ashwin, C., Baron-Cohen, S., Wheelwright, S., O'Riordan, M., Bullmore, E.T., 2007. Differential activation of the amygdala and the "social brain" during fearful face-processing in Asperger syndrome. *Neuropsychologia* 45, 2–14.
- Barnea-Goraly, N., Kwon, H., Menon, V., Eliez, S., Lotspeich, L., Reiss, A.L., 2004. White matter structure in autism: preliminary evidence from diffusion tensor imaging. *Biol. Psychiatry* 55, 323–326.
- Bishop, D.V., Norbury, C.F., 2005. Executive functions in children with communication impairments, in relation to autistic symptomatology. 2: response inhibition. *Autism* 9, 29–43.
- Biswal, B., Yetkin, F.Z., Haughton, V.M., Hyde, J.S., 1995. Functional connectivity in the motor cortex of resting human brain using echo-planar MRI. *Magn. Reson. Med.* 34, 537–541.
- Blair, J.R., Spreen, O., 1989. Predicting premorbid IQ: a revision of the National Adult Reading Test. *Clin. Neuropsychol.* 3, 129–136.

- Brown, M.R., Goltz, H.C., Vilis, T., Ford, K.A., Everling, S., 2006. Inhibition and generation of saccades: rapid event-related fMRI of prosaccades, antisaccades, and nogo trials. *Neuroimage* 33, 644–659.
- Buckner, R.L., Goodman, J., Burack, M., Rotte, M., Koutstaal, W., Schacter, D., et al., 1998. Functional-anatomic correlates of object priming in humans revealed by rapid presentation event-related fMRI. *Neuron* 20, 285–296.
- Buckner, R.L., Andrews-Hanna, J.R., Schacter, D.L., 2008. The brain's default network: anatomy, function, and relevance to disease. *Ann. N. Y. Acad. Sci.* 1124, 1–38.
- Burock, M.A., Dale, A.M., 2000. Estimation and detection of event-related fMRI signals with temporally correlated noise: a statistically efficient and unbiased approach. *Hum. Brain Mapp.* 11, 249–260.
- Bush, G., Whalen, P.J., Rosen, B.R., Jenike, M.A., McInerney, S.C., Rauch, S.L., 1998. The counting stroop: an interference task specialized for functional neuroimaging—validation study with functional MRI. *Hum. Brain Mapp.* 6, 270–282.
- Bush, G., Luu, P., Posner, M.I., 2000. Cognitive and emotional influences in anterior cingulate cortex. *Trends Cogn. Sci.* 4, 215–222.
- Cherkassky, V.L., Kana, R.K., Keller, T.A., Just, M.A., 2006. Functional connectivity in a baseline resting-state network in autism. *Neuroreport* 17, 1687–1690.
- Collins, D.L., Neelin, P., Peters, T.M., Evans, A.C., 1994. Automatic 3D intersubject registration of MR volumetric data in standardized Talairach space. *J. Comput. Assist. Tomogr.* 18, 192–205.
- Connolly, J.D., Goodale, M.A., Menon, R.S., Munoz, D.P., 2002. Human fMRI evidence for the neural correlates of preparatory set. *Nat. Neurosci.* 5, 1345–1352.
- Corbetta, M., Shulman, G.L., 2002. Control of goal-directed and stimulus-driven attention in the brain. *Nat. Rev. Neurosci.* 3, 201–215.
- Cox, R.W., Jesmanowicz, A., 1999. Real-time 3D image registration for functional MRI. *Magn. Reson. Med.* 42, 1014–1018.
- Dale, A.M., 1999. Optimal experimental design for event-related fMRI. *Hum. Brain Mapp.* 8, 109–140.
- Dale, A.M., Fischl, B., Sereno, M.I., 1999. Cortical surface-based analysis. I. Segmentation and surface reconstruction. *Neuroimage* 9, 179–194.
- DeSouza, J.F., Menon, R.S., Everling, S., 2003. Preparatory set associated with prosaccades and anti-saccades in humans investigated with event-related fMRI. *J. Neurophysiol.* 89, 1016–1023.
- Devinsky, O., Morrell, M.J., Vogt, B.A., 1995. Contributions of anterior cingulate cortex to behaviour. *Brain* 118 (Pt 1), 279–306.
- Dichter, G.S., Belger, A., 2007. Social stimuli interfere with cognitive control in autism. *Neuroimage* 35, 1219–1230.
- Doricchi, F., Perani, D., Innocia, C., Grassi, F., Cappa, S.F., Bettinardi, V., et al., 1997. Neural control of fast-regular saccades and antisaccades: an investigation using positron emission tomography. *Exp. Brain Res.* 116, 50–62.
- Everling, S., Munoz, D.P., 2000. Neuronal correlates for preparatory set associated with pro-saccades and anti-saccades in the primate frontal eye field. *J. Neurosci.* 20, 387–400.
- First, M.B., Spitzer, R.L., Gibbon, M., Williams, J.B.W., 2002. Structured Clinical Interview for DSM-IV-TR Axis I Disorders, Research Version, Nonpatient Edition. Biometrics Research, New York State Psychiatric Institute, New York.
- Fischer, B., Breitmeyer, B., 1987. Mechanisms of visual attention revealed by saccadic eye movements. *Neuropsychologia* 25, 73–83.
- Fischl, B., Sereno, M.I., Dale, A.M., 1999a. Cortical surface-based analysis. II: inflation, flattening, and a surface-based coordinate system. *Neuroimage* 9, 195–207.
- Fischl, B., Sereno, M.I., Tootell, R.B.H., Dale, A.M., 1999b. High-resolution intersubject averaging and a coordinate system for the cortical surface. *Hum. Brain Mapp.* 8, 272–284.
- Fischl, B., van der Kouwe, A., Destrieux, C., Halgren, E., Segonne, F., Salat, D.H., et al., 2004. Automatically parcellating the human cerebral cortex. *Cereb. Cortex* 14, 11–22.
- Ford, K.A., Goltz, H.C., Brown, M.R., Everling, S., 2005. Neural processes associated with antisaccade task performance investigated with event-related fMRI. *J. Neurophysiol.* 94, 429–440.
- Ford, K.A., Gati, J.S., Menon, R.S., Everling, S., 2009. BOLD fMRI activation for anti-saccades in nonhuman primates. *Neuroimage* 45, 470–476.
- Fox, M.D., Snyder, A.Z., Vincent, J.L., Corbetta, M., Van Essen, D.C., Raichle, M.E., 2005. The human brain is intrinsically organized into dynamic, anticorrelated functional networks. *Proc. Natl. Acad. Sci. U. S. A.* 102, 9673–9678.
- Gaymard, B., Rivaud, S., Cassarini, J.F., Dubard, T., Rancurel, G., Agid, Y., Pierrot-Deseilligny, C., 1998. Effects of anterior cingulate cortex lesions on ocular saccades in humans. *Exp. Brain Res.* 120, 173–183.
- Geschwind, D.H., 2009. Advances in autism. *Annu. Rev. Med.* 60, 367–380.
- Geurts, H.M., Verte, S., Oosterlaan, J., Roeyers, H., Sergeant, J.A., 2004. How specific are executive functioning deficits in attention deficit hyperactivity disorder and autism? *J. Child Psychol. Psychiatry* 45, 836–854.
- Gitelman, D.R., Nobre, A.C., Parrish, T.B., LaBar, K.S., Kim, Y.H., Meyer, J.R., Mesulam, M., 1999. A large-scale distributed network for covert spatial attention: further anatomical delineation based on stringent behavioural and cognitive controls. *Brain* 122, 1093–1106.
- Goldberg, M.C., Lasker, A.G., Zee, D.S., Garth, E., Tien, A., Landa, R.J., 2002. Deficits in the initiation of eye movements in the absence of a visual target in adolescents with high functioning autism. *Neuropsychologia* 40, 2039–2049.
- Goldberg, M.C., Mostofsky, S.H., Cutting, L.E., Mahone, E.M., Astor, B.C., Denckla, M.B., Landa, R.J., 2005. Subtle executive impairment in children with autism and children with ADHD. *J. Autism Dev. Disord.* 35, 279–293.
- Gomot, M., Bernard, F.A., Davis, M.H., Belmonte, M.K., Ashwin, C., Bullmore, E.T., Baron-Cohen, S., 2006. Change detection in children with autism: an auditory event-related fMRI study. *Neuroimage* 29, 475–484.
- Hall, G.B., Szechtman, H., Nahmias, C., 2003. Enhanced salience and emotion recognition in Autism: a PET study. *Am. J. Psychiatry* 160, 1439–1441.
- Hallett, P.E., 1978. Primary and secondary saccades to goals defined by instructions. *Vision Res.* 18, 1279–1296.
- Happe, F., Ronald, A., Plomin, R., 2006. Time to give up on a single explanation for autism. *Nat. Neurosci.* 9, 1218–1220.
- Haznedar, M.M., Buchsbaum, M.S., Metzger, M., Solimando, A., Spiegel-Cohen, J., Hollander, E., 1997. Anterior cingulate gyrus volume and glucose metabolism in autistic disorder. *Am. J. Psychiatry* 154, 1047–1050.
- Haznedar, M.M., Buchsbaum, M.S., Wei, T.C., Hof, P.R., Cartwright, C., Bienstock, C.A., Hollander, E., 2000. Limbic circuitry in patients with autism spectrum disorders studied with positron emission tomography and magnetic resonance imaging. *Am. J. Psychiatry* 157, 1994–2001.
- Henderson, H., Schwartz, C., Mundy, P., Burnette, C., Sutton, S., Zahka, N., Pradella, A., 2006. Response monitoring, the error-related negativity, and differences in social behavior in autism. *Brain Cogn.* 61, 96–109.
- Hill, E.L., 2004. Executive dysfunction in autism. *Trends Cogn. Sci.* 8, 26–32.
- Hollingshead, A.B., 1965. Two factor index of social position. Yale University Press, New Haven, Conn.
- Huerta, M.F., Krubitzer, L.A., Kaas, J.H., 1987. Frontal eye field as defined by intracortical microstimulation in squirrel monkeys, owl monkeys, and macaque monkeys. II. Cortical connections. *J. Comp. Neurol.* 265, 332–361.
- Hunt, A.R., Kingstone, A., 2003. Covert and overt voluntary attention: linked or independent? *Brain Res. Cogn. Brain Res.* 18, 102–105.
- Johnston, K., Levin, H.M., Koval, M.J., Everling, S., 2007. Top-down control-signal dynamics in anterior cingulate and prefrontal cortex neurons following task switching. *Neuron* 53, 453–462.
- Just, M.A., Cherkassky, V.L., Keller, T.A., Minshew, N.J., 2004. Cortical activation and synchronization during sentence comprehension in high-functioning autism: evidence of underconnectivity. *Brain* 127, 1811–1821.
- Kana, R.K., Keller, T.A., Minshew, N.J., Just, M.A., 2007. Inhibitory control in high-functioning autism: decreased activation and underconnectivity in inhibition networks. *Biol. Psychiatry* 62, 198–206.
- Kennedy, D.P., Courchesne, E., 2008. The intrinsic functional organization of the brain is altered in autism. *Neuroimage* 39, 1877–1885.
- Kennedy, D.P., Redcay, E., Courchesne, E., 2006. Failing to deactivate: resting functional abnormalities in autism. *Proc. Natl. Acad. Sci. U. S. A.* 103, 8275–8280.
- Klein, C., Foerster, F., 2001. Development of prosaccade and antisaccade task performance in participants aged 6 to 26 years. *Psychophysiology* 38, 179–189.
- Klein, R., McCormick, P., 1989. Covert visual orienting: hemifield-activation can be mimicked by zoom lens and midlocation placement strategies. *Acta Psychol. (Amst.)* 70, 235–250.
- Kleinhans, N., Akshoomoff, N., Delis, D.C., 2005. Executive functions in autism and Asperger's disorder: flexibility, fluency, and inhibition. *Dev. Neuropsychol.* 27, 379–401.
- Kleinhans, N.M., Richards, T., Sterling, L., Stegbauer, K.C., Mahurin, R., Johnson, L.C., et al., 2008. Abnormal functional connectivity in autism spectrum disorders during face processing. *Brain* 131, 1000–1012.
- Koski, L., Paus, T., 2000. Functional connectivity of the anterior cingulate cortex within the human frontal lobe: a brain-mapping meta-analysis. *Exp. Brain Res.* 133, 55–65.
- Koyama, M., Hasegawa, I., Osada, T., Adachi, Y., Nakahara, K., Miyashita, Y., 2004. Functional magnetic resonance imaging of macaque monkeys performing visually guided saccade tasks: comparison of cortical eye fields with humans. *Neuron* 41, 795–807.
- London, E., 2007. The role of the neurobiologist in redefining the diagnosis of autism. *Brain Pathol.* 17, 408–411.
- Lopez, B.R., Lincoln, A.J., Ozonoff, S., Lai, Z., 2005. Examining the relationship between executive functions and restricted, repetitive symptoms of autistic disorder. *J. Autism Dev. Disord.* 35, 445–460.
- Lord, C., Rutter, M., DiLavore, P.C., Risi, S., 1999. Autism Diagnostic Observation Schedule—WPS (ADOS-WPS). Western Psychological Services, Los Angeles, CA.
- Luna, B., Doll, S.K., Hegedus, S.J., Minshew, N.J., Sweeney, J.A., 2007. Maturation of executive function in autism. *Biol. Psychiatry* 61, 474–481.
- Mahone, E.M., Powell, S.K., Loftis, C.W., Goldberg, M.C., Denckla, M.B., Mostofsky, S.H., 2006. Motor persistence and inhibition in autism and ADHD. *J. Int. Neuropsychol. Soc.* 12, 622–631.
- Manoach, D.S., Weintraub, S., Daffner, K.R., Scinto, L.F., 1997. Deficient antisaccades in the social-emotional processing disorder. *Neuroreport* 8, 901–905.
- Manoach, D.S., Lindgren, K.A., Cherkasova, M.V., Goff, D.C., Halpern, E.F., Intriligator, J., Barton, J.J.S., 2002. Schizophrenic subjects show deficient inhibition but intact task-switching on saccadic tasks. *Biol. Psychiatry* 51, 816–826.
- Manoach, D.S., Lindgren, K.A., Barton, J.J., 2004. Deficient saccadic inhibition in Asperger's disorder and the social-emotional processing disorder. *J. Neurol. Neurosurg. Psychiatry* 75, 1719–1726.
- Manoach, D.S., Thakkar, K.N., Cain, M.S., Polli, F.E., Edelman, J.A., Fischl, B., Barton, J.J., 2007. Neural activity is modulated by trial history: a functional magnetic resonance imaging study of the effects of a previous antisaccade. *J. Neurosci.* 27, 1791–1798.
- Margulies, D.S., Kelly, A.M., Uddin, L.Q., Biswal, B.B., Castellanos, F.X., Milham, M.P., 2007. Mapping the functional connectivity of anterior cingulate cortex. *Neuroimage* 37, 579–588.
- Matsuda, T., Matsuura, M., Ohkubo, T., Ohkubo, H., Matsushima, E., Inoue, K., et al., 2004. Functional MRI mapping of brain activation during visually guided saccades and antisaccades: cortical and subcortical networks. *Psychiatry Res.* 131, 147–155.
- Mesulam, M.-M., 1981. A cortical network for directed attention and unilateral neglect. *Ann. Neurol.* 10, 309–325.
- Mesulam, M.M., 1990. Large-scale neurocognitive networks and distributed processing for attention, language, and memory. *Ann. Neurol.* 28, 597–613.
- Miezin, F.M., Maccotta, L., Ollinger, J.M., Petersen, S.E., Buckner, R.L., 2000. Characterizing the hemodynamic response: effects of presentation rate, sampling procedure,

- and the possibility of ordering brain activity based on relative timing. *Neuroimage* 11, 735–759.
- Milea, D., Lehericy, S., Rivaud-Pechoux, S., Duffau, H., Lobel, E., Capelle, L., et al., 2003. Antisaccade deficit after anterior cingulate cortex resection. *Neuroreport* 14, 283–287.
- Miller, E.K., Cohen, J.D., 2001. An integrative theory of prefrontal cortex function. *Annu. Rev. Neurosci.* 24, 167–202.
- Minshew, N.J., Luna, B., Sweeney, J.A., 1999. Oculomotor evidence for neocortical systems but not cerebellar dysfunction in autism. *Neurology* 52, 917–922.
- Mitz, A.R., Godschalk, M., 1989. Eye-movement representation in the frontal lobe of rhesus monkeys. *Neurosci. Lett.* 106, 157–162.
- Moore, T., Armstrong, K.M., Fallah, M., 2003. Visuomotor origins of covert spatial attention. *Neuron* 40, 671–683.
- Morecraft, R.J., Geula, C., Mesulam, M.M., 1993. Architecture of connectivity within a cingulo-fronto-parietal neurocognitive network for directed attention. *Arch. Neurol.* 50, 279–284.
- Mosconi, M.W., Kay, M., D'Cruz, A.M., Seidenfeld, A., Guter, S., Stanford, L.D., Sweeney, J.A., 2009. Impaired inhibitory control is associated with higher-order repetitive behaviors in autism spectrum disorders. *Psychol. Med.* 1–8.
- Mundy, P., 2003. Annotation: the neural basis of social impairments in autism: the role of the dorsal medial-frontal cortex and anterior cingulate system. *J. Child Psychol. Psychiatry* 44, 793–809.
- Mundy, P., Sullivan, L., Mastergeorge, A.M., 2009. A parallel and distributed-processing model of joint attention, social cognition and autism. *Autism Res.* 2, 2–21.
- Munoz, D.P., Everling, S., 2004. Look away: the anti-saccade task and the voluntary control of eye movement. *Nat. Rev. Neurosci.* 5, 218–228.
- O'Driscoll, G.A., Alpert, N.M., Matthyse, S.W., Levy, D.L., Rauch, S.L., Holzman, P.S., 1995. Functional neuroanatomy of antisaccade eye movements investigated with positron emission tomography. *Proc. Natl. Acad. Sci. U. S. A.* 92, 925–929.
- Ohnishi, T., Matsuda, H., Hashimoto, T., Kunihiro, T., Nishikawa, M., Uema, T., Sasaki, M., 2000. Abnormal regional cerebral blood flow in childhood autism. *Brain* 123 (Pt 9), 1838–1844.
- Oldfield, R.C., 1971. The assessment and analysis of handedness: the Edinburgh inventory. *Neuropsychologia* 9, 97–113.
- Ozonoff, S., Strayer, D.L., 1997. Inhibitory function in nonretarded children with autism. *J. Autism Dev. Disord.* 27, 59–77.
- Pandya, D.N., Van Hoesen, G.W., Mesulam, M.M., 1981. Efferent connections of the cingulate gyrus in the rhesus monkey. *Exp. Brain Res.* 42, 319–330.
- Paus, T., 1996. Location and function of the human frontal eye-field: a selective review. *Neuropsychologia* 34, 475–483.
- Paus, T., Petrides, M., Evans, A.C., Meyer, E., 1993. Role of the human anterior cingulate cortex in the control of oculomotor, manual, and speech responses: a positron emission tomography study. *J. Neurophysiol.* 70, 453–469.
- Phillips, M.L., Drevets, W.C., Rauch, S.L., Lane, R., 2003. Neurobiology of emotion perception I: the neural basis of normal emotion perception. *Biol. Psychiatry* 54, 504–514.
- Pierrot-Deseilligny, C., Rivaud, S., Gaymard, B., Muri, R., Vermersch, A.L., 1995. Cortical control of saccades. *Ann. Neurol.* 37, 557–567.
- Pierrot-Deseilligny, C., Milea, D., Muri, R.M., 2004. Eye movement control by the cerebral cortex. *Curr. Opin. Neurol.* 17, 17–25.
- Polli, F.E., Barton, J.J., Cain, M.S., Thakkar, K.N., Rauch, S.L., Manoach, D.S., 2005. Rostral and dorsal anterior cingulate cortex make dissociable contributions during antisaccade error commission. *Proc. Natl. Acad. Sci. U. S. A.* 102, 15700–15705.
- Raymaekers, R., van der Meere, J., Roeyers, H., 2004. Event-rate manipulation and its effect on arousal modulation and response inhibition in adults with high functioning autism. *J. Clin. Exp. Neuropsychol.* 26, 74–82.
- Rommelse, N.N., Van der Stigchel, S., Sergeant, J.A., 2008. A review on eye movement studies in childhood and adolescent psychiatry. *Brain Cogn.* 68, 391–414.
- Rutter, M., Le Couteur, A., Lord, C., 2003. *Autism Diagnostic Interview—Revised*. Western Psychological Services, Los Angeles, CA.
- Schmitz, N., Rubia, K., Daly, E., Smith, A., Williams, S., Murphy, D.G., 2006. Neural correlates of executive function in autistic spectrum disorders. *Biol. Psychiatry* 59, 7–16.
- Shafritz, K.M., Dichter, G.S., Baranek, G.T., Belger, A., 2008. The neural circuitry mediating shifts in behavioral response and cognitive set in autism. *Biol. Psychiatry* 63, 974–980.
- Silk, T.J., Rinehart, N., Bradshaw, J.L., Tonge, B., Egan, G., O'Boyle, M.W., Cunnington, R., 2006. Visuospatial processing and the function of prefrontal-parietal networks in autism spectrum disorders: a functional MRI study. *Am. J. Psychiatry* 163, 1440–1443.
- Solomon, M., Ozonoff, S.J., Ursu, S., Ravizza, S., Cummings, N., Ly, S., Carter, C.S., 2009. The neural substrates of cognitive control deficits in autism spectrum disorders. *Neuropsychologia* 47, 2515–2526.
- South, M., Ozonoff, S., McMahon, W.M., 2007. The relationship between executive functioning, central coherence, and repetitive behaviors in the high-functioning autism spectrum. *Autism* 11, 437–451.
- Sweeney, J.A., Mintun, M.A., Kwee, S., Wiseman, M.B., Brown, D.L., Rosenberg, D.R., Carl, J.R., 1996. Positron emission tomography study of voluntary saccadic eye movements and spatial working memory. *J. Neurophysiol.* 75, 454–468.
- Thakkar, K.N., Polli, F.E., Joseph, R.M., Tuch, D.S., Hadjikhani, N., Barton, J.J., Manoach, D.S., 2008. Response monitoring, repetitive behaviour and anterior cingulate abnormalities in autism spectrum disorders (ASD). *Brain* 131, 2464–2478.
- Thesen, S., Heid, O., Mueller, E., Schad, L.R., 2000. Prospective acquisition correction for head motion with image-based tracking for real-time fMRI. *Magn. Reson. Med.* 44, 457–465.
- Van Dijk, K.R.A., Hedden, T., Venkataraman, A., Evans, K.C., Lazar, S.W., Buckner, R.L., in press. Functional connectivity MRI: Theory, properties, and optimization. *J. Neurophys.*
- Vincent, J.L., Snyder, A.Z., Fox, M.D., Shannon, B.J., Andrews, J.R., Raichle, M.E., Buckner, R.L., 2006. Coherent spontaneous activity identifies a hippocampal-parietal memory network. *J. Neurophysiol.* 96, 3517–3531.
- Wang, Y., Matsuzaka, Y., Shima, K., Tanji, J., 2004. Cingulate cortical cells projecting to monkey frontal eye field and primary motor cortex. *Neuroreport* 15, 1559–1563.
- Wechsler, D., 1999. *Wechsler Abbreviated Scale of Intelligence*. The Psychological Corporation, San Antonio, TX.
- Whalen, P.J., Bush, G., McNally, R.J., Wilhelm, S., McInerney, S.C., Jenike, M.A., Rauch, S.L., 1998. The emotional counting Stroop paradigm: a functional magnetic resonance imaging probe of the anterior cingulate affective division. *Biol. Psychiatry* 44, 1219–1228.
- White, K., Ashton, R., 1976. Handedness assessment inventory. *Neuropsychologia* 14, 261–264.